EXAMINATION OF DEGRADATION FREQUENTLY REPAIRED SHEARING AND FORMING TOOLS

JOSEF IZAK, MARIAN SIGMUND

FSI VUT Brno, Faculty of Mechanical Engineering, Institute of Welding and Surface Treatments, Brno, Czech Republic

The article describes the renovation of repeatedly worn shearing tools working cold up to 200 °C. The material from which the cutting punch is made of carries the trade name CALDIE. It is delivered from the smelter in the condition after soft annealing and subsequently it is refined. A worn or damaged edge is chamfered and welded afterwards by technology of micro-TIG in pulse mode. To restore the geometry of the damaged edge is used an intermediate layer between the base material and the final hard layer the ferritic-austenitic wire Cronitex RC 220. Eventually, the final hard layer is welded to the intermediate layer, either Cronitex RC 60 or RC 63. After welding, the tool is machined to the required dimensions and then integrated back into production. The main goal was to evaluate the possibility of extending the life of cutting tools and reducing the implementation of already inefficient repairs. For assessment several destructive tests were performed - macrostructure, microstructure, microhardness measurement and EDS analysis.

KEYWORDS

Tool steel, CALDIE, renovation, lifespan, micro – TIG, weldability, Cronitex RC 220, RC 60, RC 63

1 INTRODUCTION

Nowadays, metallurgical processes are at such a high level that, thanks to controlled rolling, AHSS steels with a strength higher than 1200 MPa can be produced. Due to this, it is also necessary to produce tools that these high-strength steels will be able to form (cut, bend, etc.). The problem occurs when the tool is damaged (deformed). The production of a new tool is unprofitable and therefore the forming tools are renovated (repeatedly) using TIG technology. The basic material that is welded on is stainless tool steel. High demands are placed on its weldability - adherence to the welding procedure, the amount of heat input (internal stress and deformation), preheating, tempering of the base material (change of structure and dimensions), increase of heat affected zone (HAZ), etc., which is related to the resulting requirements after welding - high hardness 60 - 62 HRC, strength with good toughness, dimensional stability, and tool life.

2 WELDED COMPONENT

The welded part of the cutting punch, which was the subject of analysis in the article, can be seen in Fig. 3. The inclusion of a part of the cutting punch in the cutting punch can be seen in Figure 2. The whole cutting punch was part of the block of the progressive shearing tool, which can be seen in Fig. 1. It is then placed in the so-called "transfer" press and gradually forms the sheet metal into the final form of the required component. The main dimensions of the cutting punch part (hereinafter only the cutter) are 110 x 90 x 75 mm.

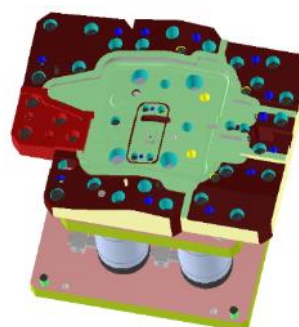**Figure 1.** Progressive shearing tool [PWO 2021].
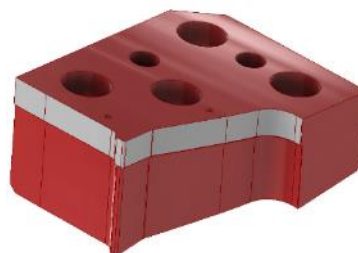

Figure 2. Cutting punch [PWO 2021].

Figure 3. Part of cutting punch [PWO 2021].

3 BASED MATERIAL AND WELDING TECHNOLOGY

3.1 Based material used

The welded base material (BM) was Cr-Mo-V CALDIE steel from Uddeholm company. It is a medium-alloy tool steel designed for cold work. As far as conventional tool steel production, CADLIE is a leader in steel development, thanks to its structure and properties. There is no significant carbide linearity, as in previously high-alloyed (ledeburites) tool steels due to the reduction of carbon content and alloying elements (especially chromium). It achieves high hardness (strength) and has high resistance to wear, breakage, and cracking.

After the heat treatment, soft annealing, which is performed above the A1 temperature (more precisely to the temperature of 820 ° C), it is already supplied from the smelters. After equilibration, it is cooled at a rate of 10 ° C / hour to a temperature of 650 ° C in an oven. Afterwards it is cooled freely in air. The structure consists of ferrite (low content of C and alloying elements) and dispersed secondary carbides, which is a suitable structure for subsequent machining into the desired tool shape [UDDEHOLM 2019].

To achieve the useful properties, a hardening operation and then tempering to secondary hardness follow.

Due to the low thermal conductivity of tool steels, heating to the austenitization temperature is performed in stages. The delays are used to balance the temperatures between the surface and the core, so that there is no stress and deformation of the tool. The individual delays are at temperatures of 650 ° C and 850 ° C. The delay time is approximately 1 hour. The hardening temperature is 1070 ° C (endurance 0.5 - 1 hour depending on the size of the tool), when the primary (partially) and secondary carbides are converted to austenite and dissolved. This is followed by quenching and transformation of austenite to tetragonal martensite. The cooling rate is 1 ° C / s (according to the ARA diagram) to a temperature of 50 ° C [UDDEHOLM 2019].

Immediately after hardening, tempering to secondary hardness follows. The aim of tempering is to reduce the contribution of residual austenite (A_Z) and increase the amount of secondary precipitated carbides.

To remove a residual austenite multiple tempering is required. Residual austenite begins to transform into martensite when the M_S temperature is reached. To achieve the transformation of all austenite to martensite, a temperature M_f below room temperature must be reached. Alternatively, residual austenite may transform during tempering because precipitation of carbides during tempering reduces the amount of carbon and alloying elements in the solid solution, thereby increasing the temperature M_f. After cooling, part or all the A_Z transforms into martensite. The transformation of residual austenite to martensite is desirable because the proportion of A_Z in the structure can lead to dimensional changes. After the first tempering, the structure consists not only of tempered martensite, but also of fresh martensite. Even a small amount of fresh martensite can affect the overall toughness of the tool. For this reason, it is recommended to temper multiple times. The tool is tempered to a secondary hardness a total of 5 times, at a temperature of 525 ° C. The hardening and tempering scheme can be seen in Figure 4 [RAFAEL 2016].
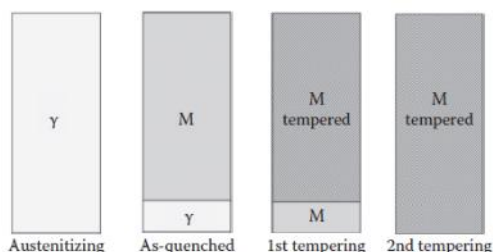

Figure 4. The principle of hardening and tempering [RAFAEL 2016].

During precipitation, the lattice of martensite gradually changes from tetragonal to cubic and carbon diffuses from martensite. Carbon, together with alloying elements (Cr, Mo, V), forms carbides such as M_7c_3, M_2C and MC (M_4c_3). Secondary carbides prevent the movement of dislocations, thus increasing the strength of the tool. Carbides also have a beneficial effect on the wear resistance of the tool. Figure 5 shows the types of carbides formed at 525 ° C during tempering to secondary hardness. The achieved hardness of primary and secondary carbides can be seen in Figure 6 [RAFAEL 2016].
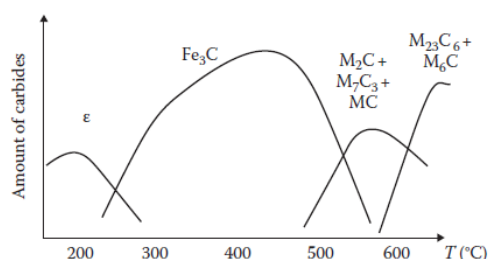

Figure 5. Precipitation of carbides during a tempering [RAFAEL 2016].
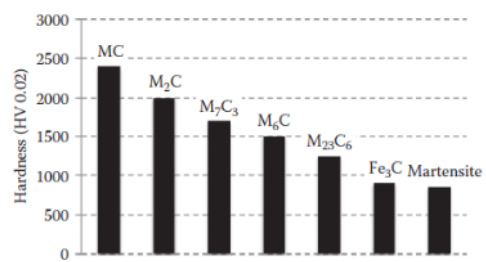

Figure 6. Carbide hardness [RAFAEL 2016].

The chemical composition of tool steel CALDIE and the mechanical properties are presented in Tables 1 and 2.

C	Si	Mn	Cr	Mo	V	P, S
0.73	0.21	0.49	4.99	2.32	0.51	<0.005

Table 1. Chemical composition in wt. % of tool steel CALDIE.

$R_{c0,2}$ [MPa]	HRC
2430	61

Table 2. Mechanical properties of tool steel CALDIE [UDDEHOLM 2019].

3.2 Filler materials used (wire)

For welding a heterogeneous joint, i.e., the base material and the final hard filler material (FM), it is not appropriate to use a so-called "hard to hard" connection. Both materials contain relatively high amounts of carbon and alloying elements. In the transition area, stress, cracks and even delamination of the weld can occur. For this reason, it is advisable to use austenitic wire between the base material and the final hard layer, which guarantees a good metallurgical connection of both filler materials, and the risk of cracks is thus eliminated completely. The method of laying beads can be seen in Figure 7.

Figure 7. Method of laying beads [ESAB 2011].

CRONITEX RC 220 is a high-alloy wire with a ferritic-austenitic (duplex) structure. It is used, as an intermediate layer, in the welding of tool steel forming tools. It is a tough material that prevents the formation and propagation of cracks during joining. The chemical composition of CRONITEX RC 220 wire and the mechanical properties can be seen in Tables 3 and 4.

C	Cr	Mn	Mo	Ni	Si	V	Fe
0.1	30.5	1.9	0.5	10.0	0.6	0,3	Rest.

Table 3. Chemical composition of CRONITEX RC 220 wire.

R_m [MPa]	HV	A [%]
840	235	29

Table 4. Mechanical properties of CRONITEX RC 220 wire.

There are two types of final hard filler materials CRONITEX RC 60 or RC63. In both cases, the wires are so-called self-hardening in air after welding and after the welding process they should reach a hardness of 60 - 62 HRC. The chemical composition of CRONITEX RC 60 wire and the mechanical properties are shown in Tables 5 and 6.

C	Cr	Mn	Mo	Si	V	Fe
0.4	7.2	1.3	1.8	0.4	0.3	Rest.

Table 5. Chemical composition CRONITEX RC 60 wire.

Hardness after welding 2 layers [HV]	680
With intermediate layer [HV]	720

Table 6. Mechanical properties CRONITEX RC 60 wire.

CRONITEX RC 63 should achieve higher hardness and better excluded structures after welding. The chemical composition of the wire and the mechanical properties are shown in Tables 7 and 8.

C	Cr	Mn	Mo	Si	V	Fe
0.6	6.8	0.5	1.7	1.0	0.6	Rest.

Table 7. Chemical composition CRONITEX RC 63 wire.

Hardness after welding [HV]	680 – 750

Table 8. Mechanical properties CRONITEX RC 63 wire.

3.3 Surfacing overlay welding technology used

For renovation of forming tools from tool steel, it is an important requirement that the temperature be high enough to melt the filler material and that there is no high heat input. Since too high a temperature, the base material is tempered, which leads to its degradation, the HAZ expands, and the tool is deformed. As a result, the dimensions of the tool change due to a change in the structure of the base material. For this reason, micro - TIG technology in pulse mode was used for welding shearing edges. The frequency of the current pulse change was 120 Hz (pulse distribution 50/50). The shielding gas was high purity argon 4.6. The gas flow was 6 l / min. All samples were welded with a tungsten electrode WL 20 with a diameter of 1.6 mm, angle 15 °. The individual sample welding parameters can be seen in Table 9.

Sample	Base current I_Z [A]	Impulse current I_P [A]	Weld. voltage U [V]
Sample No. 1 (RC60)	50 – 60	3	10 – 12
Sample No. 2 (RC63)	47 – 60	10	10 – 12
Samples No. 3, 4, 5	60 – 65	10	10 – 12

Table 9. Welding parameters of individual samples.

Sample No. 1 (RC 60) and No. 2 (RC 63) were welded in the same way in terms of laying beads. First, an intermediate layer (RC 220) was welded and then two final beads of hard filler material were welded. In the case of sample No. 1, wire RC 60 and sample No. 2 filler material RC 63 were welded. Sample RC 60 was an intermediate layer, and the first layer was welded with direct current and the second layer with pulsed current. In the RC 63 sample, the intermediate layer was welded with direct current and the other layers with pulsed current. The heat input was calculated as the arithmetic average of the heat input contributions from individual beads. The amount of heat introduced can be seen for individual samples in Table 10.

Sample	RC 60	RC 63
Heat input Q_V [kJ/mm]	0.34	0.28

Table 10. Amount of heat input.

For sample No. 3, 4, 5, the number of times the individual passages were welded was monitored. Renovated several times with RC 220 and RC 60 (RC 63). For simplicity, you can see the sample designation and the number of welds in the Table 11 (for example Corner 5x).

Table 11. Sample designation depending on the number of welds.

Sample No. 3	Sample No. 4	Sample No. 5
Radius 2x	Middle 3x	Corner 5x

4 EXPERIMENTAL PART

4.1 Position of metallographic samples

To produce samples No. 1 (RC 60) and No. 2 (RC 63), the cutting punch was first cut into two parts using EDM technology due to the smallest possible heat affected zone. Figure 8 shows how the section was made. The individual sampling locations can be observed in Figure 9.

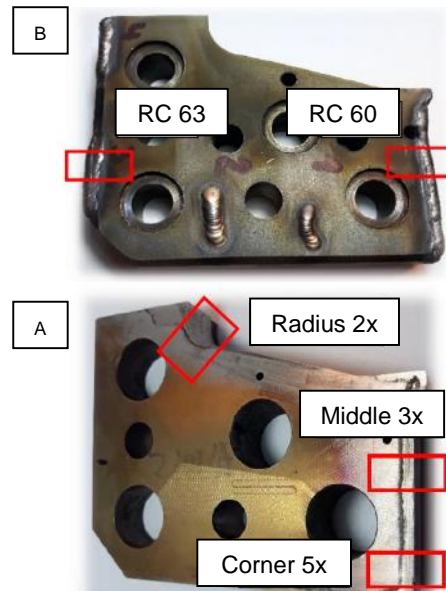**Figure 8.** Section of cutting punch.

Figure 9. Sampling locations.

4.2 Evaluation of macrostructure

For etching the structure Villela is used ($C_6H_3N_3O_7$ + HCl + C_2H_5OH). Subsequently, Nital (3% HNO_3 in ethanol) was used.

Here is a legend for better orientation and easier identification of individual passages in the deposit:

- A – Based material (BM),
- B – heat affected zone (HAZ),
- C – dilution area of BM and intermediate layer,
- D – intermediate layer (IL),
- E – dilution area of IL and final weld metal,
- F – weld metal (WM).

At first, RC 60 and RC 63 were evaluated, where a history of welding is known. In Figures 10, 11, 12 a deposit with an intermediate layer and two final beads can be observed. In both cases, preheating was not included, but it was partially represented by welding the IL. At first sight, it was not possible to accurately identify the laying beads.

In Fig. 10, at the weld deposit FM RC 60 was used. The width of the HAZ is approximately 2 mm. There are scratches above caused by inconsistent grinding when making a sample. In terms of defects, there are two bubbles or shrinkage cavity at the top. In the blue marked area, you can see a groove through the weld. This is a brighter spot and will probably be a melting point, or touch of the tungsten electrode, when placing the beads.

Figure 10. Macrostructure RC 60, magnification 25,6.

In Figures 11 and 12, FM RC 63 was used as the final layer. The width of the heat affected zone is approximately 1 mm. Compared to the previous weld deposit, its size is smaller due to the use of impulse current, which is also proved by the calculation of the heat input. In the area of the weld deposit, only two small micro-shrink holes are found in the final layer.

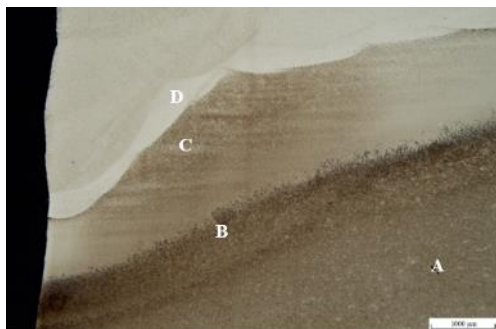**Figure 11.** Macrostructure RC 63, magnification 25,6x.

Figure 12. Macrostructure RC 63, magnification 25,6x.

In both cases, due to the austenitic intermediate layer, there is a good metallurgical connection of the welding beads, no cracks or imperfect connection of the beads in the dilution area. Defects in the form of bubbles and shrink cavity do not affect the final function of the cutting tool.

Samples No. 3, 4, 5 were subjected to multiple welding, after deformation of the cutting edge. Even the last welded passages were put into operation before the cutting punch was scrapped. The preheating to 250 °C was included in all cases before welding. Due to the impossibility of capturing the entire renovated area with a microscope, the most stressed place (cutting edge) was chosen. The HAZ was variable in all three cases. The largest was in the upper area of the weld deposit.

In Figure 13, it was observed a microstructure, which was welded twice. The width of the HAZ is approximately 1.2 mm. A tine defect can be observed in the blue marked area.

Figure 14 shows the renovated part, which was repaired 3 times. A size of the head affected zone was approximately 1.6 mm. In the deposit there were identified no visible defects.

In Figure 15, it was observed a microstructure, which was renovated 5 times. The heat affected zone was significantly larger here than in the previous samples. The width of the heat affected zone was approximately 2 mm. Something that could correspond to a crack indication can be seen in the blue marked area. However, the shape and nature of the spread is very peculiar and will be something else ("possible primary grain boundary").
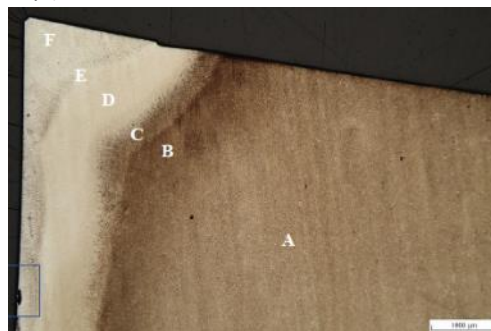

Figure 13. Macrostructure radius 2x, magnification 25,6x.

Figure 14. Macrostructure middle 3x, magnification 25,6x.
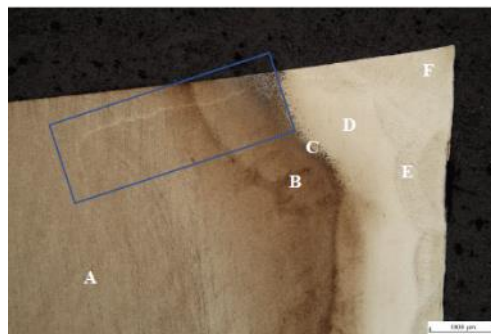

Figure 15. Macrostructure corner 5x, magnification 25,6x.

In the welds there were not any defects which would affect the function of the cutting punch. Looking at BM, you can see how it was shaped according to the bright places that repeat regularly in the lines. From the point of view of the influence of carbide linearity, the tool was suitably oriented, because it achieves the best strength properties just when the direction of the cut was parallel to the forming structure.

4.3 Evaluation of microstructure

The evaluation of the microstructure was realized mainly on a sample marked RC 60 (sample No. 1). In most cases, the Cronitex RC 220 and RC 60 configurations was used during welding. Later, the figures show that the structure of the FM RC 63 was very similar to the wire RC 60. Figure 16 shows the positions where the microstructure image was taken. The etching was of two kinds. For better orientation, the type of etching is indicated in the description of the image:

- (1) Villela and then Nital
- (2) Villela + HCl

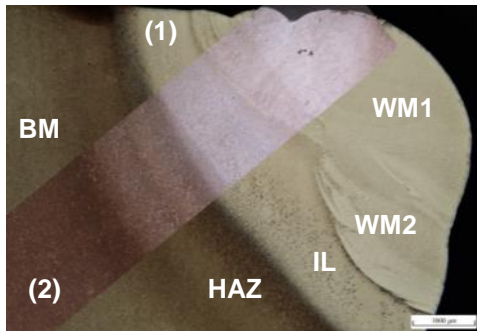Figure 16 shows the individual marked sites that are observed on the microstructure.

Figure 16. Positions of microstructure RC 60, magnification 25,6x.

The structure of the base material consisted of martensite, residual austenite and a certain amount of carbides. The most common type of carbide in the structure was the M_7C_3 type, most commonly chromium. Due to the chemical composition, M_2C carbide, mostly molybdenum, also may be present in the structure. To a lesser extent, MC-type carbides (M_4C_3), which were most often vanadium, will appear in the structure. Chromium carbides was likely to be of the secondary type as it dissolves at lower temperatures (500 – 600 °C). Molybdenum carbides, and especially vanadium, can be both primary and secondary. Due to the multiple tempering, no amount of A_Z can be seen in the structure at first sight. Figure 17 shows a sample structure of what most of the BM looks like. The distribution of carbides was homogeneous and no significant carbide linearity was formed, which has a positive effect on mechanical properties and weldability.
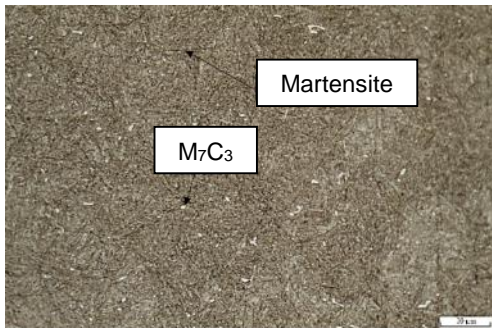

Figure 17. Microstructure BM, RC 60, magnification 1000x, (1).

Figure 18. Microstructure HAZ, RC 60, magnification 1000x, (1).

In Figure 18, we can see the microstructure of HAZ. Looking at the structure, it is very likely a coarse plate martensite with a relatively high proportion of residual austenite. The reason should be the diffusion of nickel during melting into BM, where plate martensite was being formed. Residual austenite was tough, but there was also a high proportion of plate martensite. If stress would be created during welding, microcracks may form, initiate, and reduce the life of the weld deposit.

In Figure 19, this transition can be observed at lower magnification. The area of the plate martensite in the case of this weld deposit was approximately 550 µm.

Figure 17. Microstructure HAZ – IL, RC 60, magnification 250x, (1).

The structure of the IL should be duplex after welding, according to the material sheet. However, during welding, the weld pool was relatively large and there was probably a large dilution, partial diffusion of Cr and Ni into the base material and the upper final weld deposit. Nickel was not sufficient to stabilize the austenitic structure. After welding, the structure of austenite, martensite and bainite was formed along the grain boundaries (dark brown). There was also partial precipitation of carbides in the intermediate layer and the structure that was originally tough is relatively hard now. Figure 18 shows the structure of the IL upper part. Figure 19 pictures the lower part of the IL, where the "brown dots" were an etched structure of residual austenite. The evidence can be seen in Figure 20, where martensite needles "shoot" through residual austenite.

Figure 18. Microstructure IL (upper part), RC 60, mag. 1000x, (2).

Figure 19. Microstructure IL (lower part), RC 60, mag. 1000x, (2).
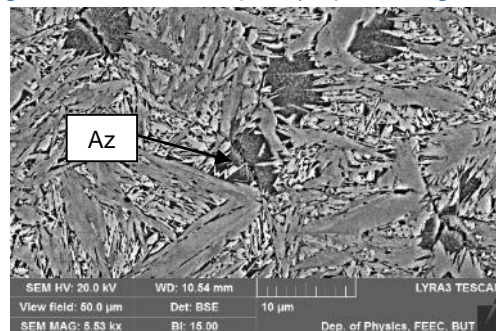

Figure 20. Microstructure IL (lower part), RC 60, mag. 5530x, (2).

Figures 21 and 22 both depict the structure after welding with the FM RC 60 and RC 63, as the final weld beads. The structure of the weld deposit should consist of martensite, a proportion of residual austenite and carbides. From the images on both structures, we can see a network forms around the martensite. This was most likely the delta ferrite phase, which is the soft phase. In the case of dynamically stressed components, the delta ferrite phase is favorable because it imparts toughness to the weld deposit and the carbides together with martensite form a sufficient hardness. In the case of a shearing tool whose application primarily requires high wear resistance, the proportion of delta ferrite is undesirable.
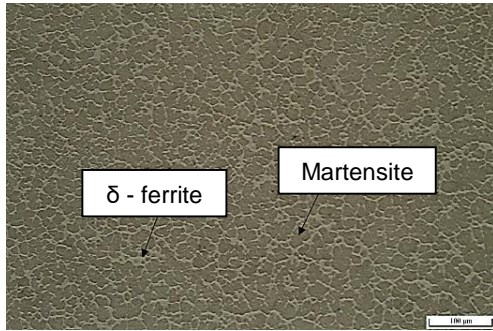

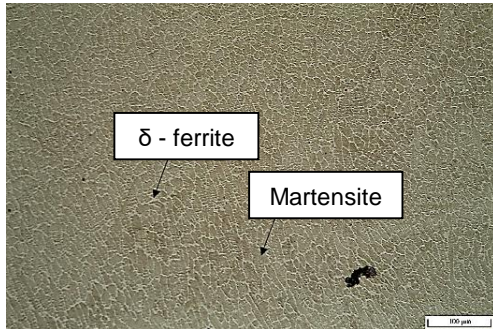**Figure 21.** Microstructure WM, RC 60, magnification 250x, (1).

Figure 22. Microstructure WM, RC 63, magnification 250x, (1).

Comparing Figures 21 and 22, we get a result that the proportion of delta ferrite was higher in the weld metal renovated with wire RC 60. From the point of view of the excluded microstructure for a given application of a shearing tool, the wire RC 63 achieves a higher quality. According to the equilibrium diagram Fe - Fe₃C, delta ferrite is stable only at high temperatures (above 1392 ° C). However, with a certain ratio of austenite-forming and ferrite-forming elements, this high temperature phase can become stable even at normal temperatures. The Fe - C - Cr diagram (8 % Cr) was used to approximate the possible delta ferrite phase in the weld metal. When carbon is plotted in the graph according to Tables 5 and 7 on the x-axis, it can be seen that the curve passes through delta ferrite areas during solidification and this structure can be eliminated in the weld deposit. The diagram is only for chromium, other ferrite-forming elements contained in the wire are not included here, which would further expand the delta ferrite zone.

Figure 23. Ternary diagram Fe − C − Cr (8 % Cr) [JURCI 2009]
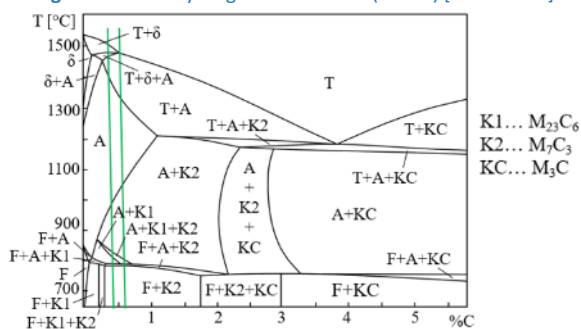
The structure of the final weld bead (WM 1 and WM 2) can be seen at higher magnification in Figures 24 and 25. In the upper area (WM 1) the structure was "polyhedral", while in the lower area (WM 2) the structure was "columnar". Everything from the melt is coarse, which was the case with delta ferrite observed in the structure.

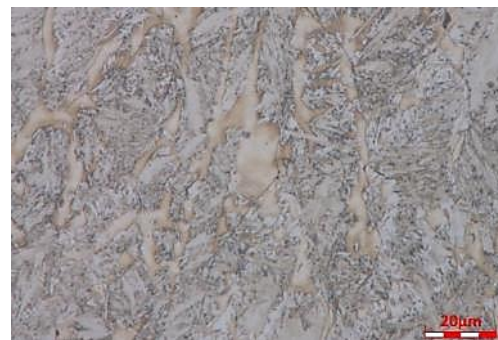**Figure 24.** Microstructure WM1, RC 60, magnification 2000x, (2).

Figure 25. Microstructure WM2, RC 60, magnification 2000x, (2).

To increase the service life of the cutting punch, the tool should be heat treated (partial austenitization + tempering to secondary hardness). This would dissolve the delta ferrite phase and the structure would then be formed by martensite with a larger amount of carbides, which would increase the wear resistance and blade grip. The problem could occur with dimensional changes of the tool during heat treatment (phase transformation).
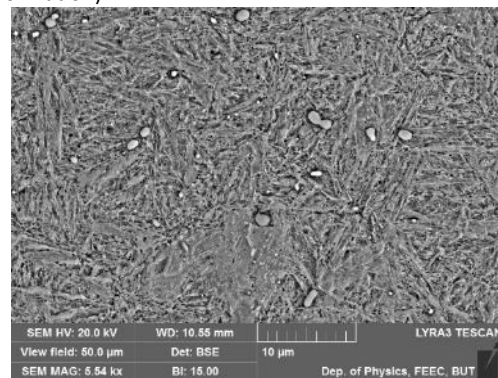

Figure 26. Microstructure BM, RC 60, magnification 5540x, (2).
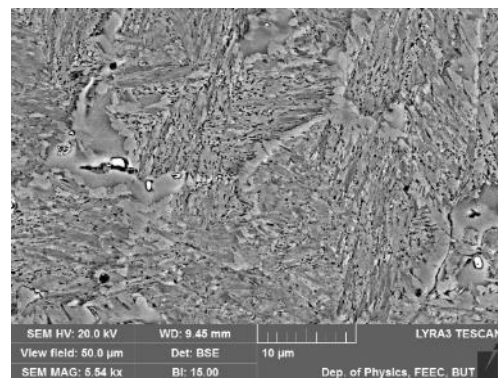

Figure 27. Microstructure WM1, RC 60, magnification 5540x, (2).

For comparison, Figure 26 shows the original structure that formed the tool geometry (martensite, a small amount of A_Z and carbides) and Figure 27 shows the tool structure after welding FM RC 60 (martensite, AZ, delta ferrite and a small amount of carbides). Thanks to the heat treatment, the "original" structure would be restored, and the tool life would be increased 2 to 3 times. Due to the size of the carbides in the BM, the homogeneous arrangement in the structure, the small proportion of A_Z, no fundamental dimensional changes should occur, and the heat treatment designed in this way would be theoretically feasible.

4.4 Vickers hardness evaluation

The microhardness test was performed on a microhardness tester Qness Q10A. The advantage is the possibility to take a picture of the puncture site after measuring the hardness. The load size was selected to be 200 g (HV 0.2). Load time was 10 s. Puncture distance was 0.2 mm.

First, the value of the final weld metal layer (WM) was measured on samples RC 60 and RC 63, whether it reaches the guaranteed hardness declared according to the material sheet. Figure 28 shows the location of the puncture line. For evaluation, 9 hardness values were measured for each weld deposit and an arithmetic average of these values was performed. The resulting value was compared with the values from the material sheet. According to Table 11, the required hardness was achieved in both cases.
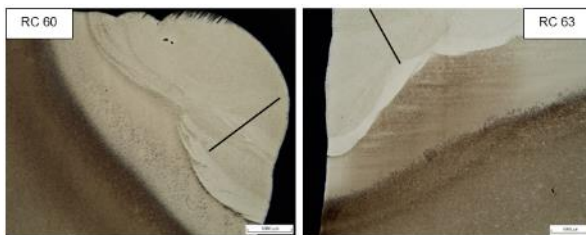

Figure 28. Location of hardness measurement lines.

Type of final weld deposit	RC 60	RC 63
Average measured hardness value [HV 0.2]	735	811
Hardness value according to the material sheet [HV]	720	680 - 740

Table 11. Comparison of the final weld deposit bead hardness.

One of the main points was to limit the implementation of inefficient repairs. For this reason, the hardness in the "sub-weld" zone was measured. Samples No. 3, 4, 5 were taken from the cutting punch after a certain number of renovations in order to find out what effect the continuous renovation of the cutting edges has on the degradation of the BM structure. For assessment, samples were taken from places after 2, 3, 5 renovations. Figure 29 shows the points where the puncture lines were drawn. The line was always drawn from the cutting edge towards the HAZ.

Figure 29. Hardness measurement line.

Figure 30 shows a graph of the measured hardness of each sample as a function of the line. When measuring the hardness, a picture of the microstructure was always taken after the indenter impression. Based on the hardness values and individual images from the puncture sites, the approximate HAZ

range was determined. Figure 30 shows where the heat-affected zone on each sample begins and where it ends. Also, we can see that with increasing number of welds, the hardness value in HAZ decreases and expands. In Table 12 are the values of the size of the heat-affected zone after subtraction from the graph.

Obviously, this cannot be applied globally, and this information can be taken as a precedent. It is affected by many other influences that are not included in the experiment, such as the extent of renovation, the effect of the current used, the welding speed, etc. The heat affected area will not expand indefinitely, but what will likely to happen is that the hardness of the BM will keep decreasing. The reason for researching this phenomenon was to create an idea of how the heat-affected zone and based material will behave during multiple welding.

Another interesting thing that can be observed already in the evaluation of the microstructure was the reinforcing effect of the intermediate layer. One of the problems was the dogma that the IL is tough, and the final hard layer must not be machined during machining so that we do not lose the hardness of the cutting edge. As can be seen from the graph, the intermediate layer strengthens significantly after welding the final hard layer.
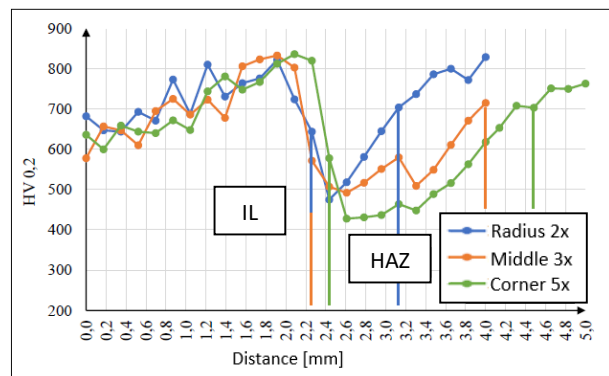

Figure 30. Hardness graph over puncture distances.

Sample	radius 2x	middle 3x	corner 5x
HAZ width [mm]	0.9	1.75	2

Table 12. HAZ size depending on the number of renovations.

Due to the scope of the article, only images of the puncture microstructure from certain passages (WM, IL, lowest hardness HAZ, BM) are placed here, in Table 13.

Table 13. Microstructure from puncture sites with microhardness tester.

4.5 EDS analysis evaluation

The aim of chemical microanalysis was to control the chemical composition and thus the given structure. In every welding process, it is necessary to create a weld pool for a good connection of materials. This can lead to dilution due to melting of BM and FM, diffusion, or carbides precipitation, etc.

During the observation of the macrostructure and microstructure, it was not possible to determine the position of the intermediate layer at first sight. When measuring the hardness, it can be seen in Figure 30 that strengthening occurs at the point where the interlayer should occur. For this reason, a chemical microanalysis was realized. The analysis was performed on samples RC 60, RC 63, and corner 5x. On samples RC 60 and corner 5x were likely to occur dilution and the IL as such was not exactly identifiable. Figure 31 shows the line analysis of sample RC 63. In Figure 32, we can see a remnant of undiluted intermediate layer. Chromium increased in the range of 300 to 800 µm. It can also be observed that the nickel dilution (diffuses) after welding into the final weld metal layer and partly into the BM. For this reason, the duplex structure was unlikely to stabilize, and the interlayer strengthens. Due to the scope of the article, only the analysis of the RC 63 sample was included here.
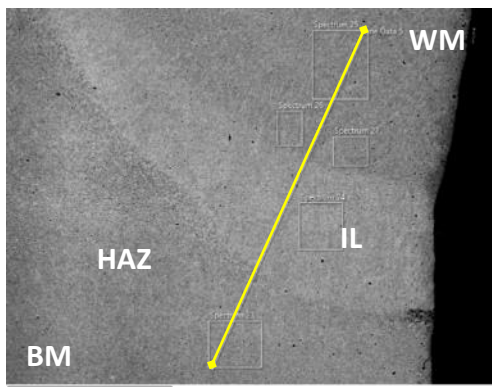

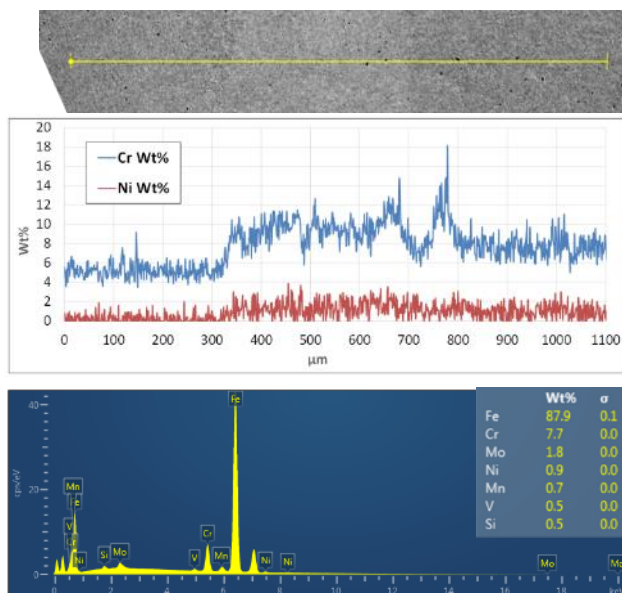
Figure 31. Line analysis, RC 63

Figure 32. EDS analysis results of sample RC 63

5 CONCLUSION

In this article the weldability of cold work tool steels was evaluated in the current state of welding. The aim was to assess possible financial savings, the possibility of extending the life of tools and reducing the implementation of already inefficient repairs.

The subject of the research was a part of the cutting punch made of CALDIE steel and after wearing it is renovated with additional materials. The wires used for the renovation were, in terms of function, the Cronitex RC 220 as intermediate layer and the final hard weld wires Cronitex RC 60 and RC 63. The renovation was carried out using micro - TIG technology. A total of 5 samples were evaluated, while 3 samples were taken directly from the functional tool after decommissioning and another two were made by the company, which is the supplier of wires. The quality of individual samples was then evaluated using destructive tests.

The first test method was to observe the macrostructure. When evaluating all samples from the macrostructure, it can be stated that no serious defects were found that would undermine the high quality of welds deposit.

Other tests that have been performed on the samples were microstructure evaluation, hardness measurement and chemical microanalysis. Since the same additional materials were used for the renovation, and thus also the excluded structures, one representative sample with the designation RC 60 was selected within the microstructure and evaluated in terms of structure. The only exception was the final weld deposit layer of filler material RC 63, which was structurally very similar to that after welding with wire RC 60. The first issue that can be noticed during the microstructure evaluation was the formation of martensite, a bainitic structure with carbides precipitated in the IL zone. The structure of plate martensite with a high proportion of residual austenite appeared in the heat-affected area. The reason could be the diffusion of nickel into the base material. Residual austenite is a tough phase, but a relatively coarse plate martensite was formed here, which can initiate cracks under stress. From the point of view of welding, this is not a very favourable structure. Due to the achieved hardness of the intermediate layer, we can say that IL was not very elastic, as guaranteed by the wire supplier. An important factor is that thanks to the intermediate layer, there is a good connection between BM and WM. It is also not necessary to take high attention to the machining of the final hard layer due to the reinforcing effect of the intermediate layer. When comparing the final weld deposit layer on samples RC 60 and RC 63, the welds deposit met the hardness declared according to the material sheet. The better quality of hardness and excluded structure after welding of wire RC 63 was also confirmed. Within samples RC 60 and RC 63 (but also sample No. 3, 4, 5) form in structure network solid solution of delta ferrite, martensite, residual austenite, and a small proportion of carbides. If the tool is stressed dynamically, the delta ferrite phase is favourable. Hardness and wear resistance are more important properties due to the application on the shearing tool, which was an analysis of the article. For this reason, it would be appropriate to heat-treat the cutting punch (partial austenitization + tempering to secondary hardness). As a result, the delta ferrite phase dissolves during austenitization. The WM structure would then be formed by martensite, and especially by a larger amount of secondary precipitated carbides. This could increase the life of the cutting punch 2 to 3 times. Problems could arise with dimensional stability of the tool, heterogeneity, enlargement of carbides in the BM and subsequent cracking of the tool during hardening. Because carbides are homogeneously dispersed in the structure of the base material (there is no significant carbide linearity) and the size of the carbides is in the range of 3 to 4 µm, the heat treatment could theoretically be feasible. Furthermore, the width of the heat-affected zone was examined based on the assessment of hardness and images from

the microstructure after puncture on samples radius 2x, a middle 3x and a corner 5x (the number indicates the number of renovations). The aim was to find out how the HAZ expands after multiple renovations of a certain passage. It is obvious that several other factors were involved, such as the size and type of current, during welding, the extent of renovation, etc. The reason for researching this phenomenon was to form an idea of how the heat-affected area will behave during multiple welding. The idea that the HAZ would grow, but not indefinitely, was confirmed. Most importantly, there was a decrease in hardness in the heat affected area. The hardness value will decrease with each subsequent welding. The solution is to machine the softened area after a certain number of welding operations. Another possibility of erasing the softened area is the already mentioned heat treatment. The welds deposit achieves high quality and good hardness after welding. In terms of price performance, micro - TIG welding technology is practically irreplaceable.

REFERENCES

[PWO 2021] PWO. Progressive shearing tool. Valasske Mezirici, Palackeho 526.

[UDDEHOLM 2019] Material sheet Caldie. Uddeholm [online]. 2019 [cit. 2021-5-20]. Available from: https://www.uddeholm.com/app/uploads/sites/49/2017/09/caldie-eng_p_0419-e20.pdf

[RAFAEL 2016] RAFAEL A. MESQUITA. *Tool Steels*. CRC Press, 2016. ISBN 9781439881712. Available from: doi:10.1201/9781315181516.

[ESAB 2011] Welding manual: Repair and maintenance. 6. updated. Vamberk: ESAB VAMBERK s.r.o., 2011.

[JURCI 2009] JURCI, Peter. Tool steel of ledeburitic type. Praha: Czech Technical University in Prague, 2009. ISBN ISBN978-80-01-04439-1.

[SIGMUND 2021] SIGMUND, M.; IZAK, J. APPLICATION OF WC GRAINS BY DEPOSITION BRAZING. *MM Science Journal,* 2021, 2021, 4, 857-4862. ISSN: 1805-0476.

[FILA 2010] FILA, P., M. BALCAR, L. MARTINEK, P. SUCHMANN, J. KREJCIK, L. JELEN a E. PSIK. DEVELOPMENT OF NEW TYPES OF TOOL STEELS DESIGNED FOR FORGING DIES. *MM Science Journal*. 2010, 222-224. ISSN 18031269. Available from: doi:10.17973/MMSJ.2010_12_201020

CONTACTS:

Ing. Josef Izak, Ing. Marian Sigmund, Ph.D.
FSI VUT Brno, Faculty of Mechanical Engineering, Institute of Welding and Surface Treatment Technology
Technicka 2896/2, Brno, 616 69, Czech Republic
+420720535501, 183119@vutbr.cz

https://www.vutbr.cz/lide/josef-izak-183119